Cite this: *Chem. Commun.*, 2011, **47**, 3583–3585

www.rsc.org/chemcomm

COMMUNICATION

Metastable state nanoparticle-enhanced Raman spectroscopy for highly sensitive detection†

Liangbao Yang,*[a] Honglin Liu,[a] Jin Wang,[a] Fei Zhou,[b] Zhongqun Tian[c] and Jinhuai Liu*[a]

Received 13th January 2011, Accepted 31st January 2011
DOI: 10.1039/c1cc10228a

Metastable state silver nanoparticle surface-enhanced Raman scattering has been experimentally and theoretically demonstrated; the signal is two to three orders of magnitude higher than that for the traditional method. Ultrasensitive surface-enhanced Raman scattering signals of illicit drug cocaine and organophosphate pesticide methyl-parathion were observed.

Understanding and controlling the assembly of colloidal particles is central to the creation of new soft materials. Routes that exploit spontaneous self-assembly in thermal nonequilibrium are more important. That is, nonequilibrium processes offer more control—because assembly is then governed not just by thermodynamic conditions but by the entire process history.[1] Moreover, the resulting materials may become trapped in deeply metastable states, remaining more robust than an equilibrium phase. The packing process of colloidal particles has been observed,[2] which is believed to solely stabilize the bicontinuous emulsions[3] and to arrest the liquid–liquid phase separation of a binary solvent.[4] The embedded nanostructure may activate an equilibrium or metastable state for the nanoisland on the top surface of a multilayered Stranski–Krastanow system.[5] One-dimensional cluster growth and branching gels in colloidal suspension systems has short-range depletion attraction and screened electrostatic repulsion,[6] and gelation in suspensions of model colloidal particles exhibits short-range attractive and long-range repulsive interactions. At low packing fractions, particles form stable equilibrium clusters; however, upon increasing the packing fraction the clusters grow in size and become increasingly anisotropic until finally associating into a fully connected network at gelation.[7] This colloidal network remains stable after thoroughly remixing, creating a new type of gel in which colloids in a single-phase solvent have locally planar coordination.[8]

Herein, we find a new metastable state of silver nanoparticle film as surface enhanced Raman spectroscopy (SERS) substrate with remixing the solvent during the volatilization process. The strategy is to just drop only 5 μL water on dry silver nanoparticles film (Fig. 1b). There is obvious evidence to prove the change of silver nanoparticles during the solvent volatilization process. Dark-field color images were collected from nanoparticles deposited on a glass wafer. Nanoparticles were illuminated by collimated white light passed through and collected by the same objective (100 × DF, numerical aperture (NA), 0.9). Scattered light was very slight purple (Fig. S2A) and light blue (Fig. S2B) from dry particles film and wet film, respectively. The colors, thus, provide a qualitative measure of the strength of interaction between nanoparticles which means that the interparticle spacing decreases.[9] During the volatilization process, the nanoparticles keep moving until the liquids have disappeared (Supplementary S2 and movie). The whole

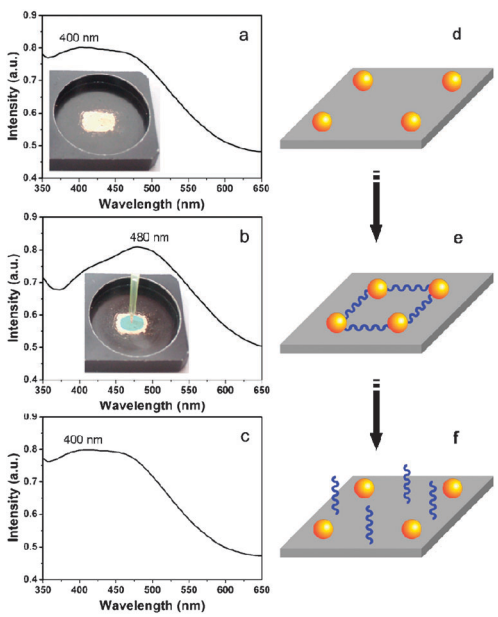

Fig. 1 Working principles of MSNERS compared to conventional dry state. a–c: UV-vis diffuse reflection absorption spectra of dry state film (a), adding water on the dry state film (b), and the film while the solvent volatilizes completely (c). d–f: Schematic of the distance between two nanospheres of dry state (d), adding water on the dry state film (e), and the film while the solvent volatilizes completely (f).

[a] *Institute of Intelligent Machines, Chinese Academy of Sciences, Hefei 230031, China. E-mail: lbyang@iim.ac.cn, jhliu@iim.ac.cn; Fax: +86-551-5592420; Tel: +86-551-5592385*
[b] *Laboratory of Optical Physics, Beijing National Laboratory for Condensed Matter Physics, Institute of Physics, Chinese Academy of Sciences, P.O. Box 603, Beijing 100190, China*
[c] *State Key Laboratory of Physical Chemistry of Solid Surfaces and Department of Chemistry, Xiamen University, Xiamen 361005, China*

† Electronic supplementary information (ESI) available: Experimental section; preparation of Ag-nanospheres; video of dynamic process; dark-field images of silver nanoparticles on dry film and adding a drop of water on dry film. See DOI: 10.1039/c1cc10228a

volatilization process takes less than five minutes. The morphologies at the end are almost the same as the original film. We can obtain the jointly enhanced Raman signal contributed by all of these metastable moving nanoparticles during the volatilization process, which is two to three orders of magnitude higher than that for the traditional dry state. We call this new technique metastable state nanoparticle-enhanced Raman spectroscopy (MSNERS). MSNERS offers several advantages compared with conventional SERS methodologies. Firstly, it describes a very simple method, where the SERS materials are extremely general and the substrate fabrication does not enjoy utmost courtesy. Secondly, it has high detection sensitivity and reproducibility due to SPR and the laser irradiation-induced automatic concentration during the detection process. Thirdly, the solvent also protects the target molecule from laser damage, at the same time, oxidation of silver nanoparticle-based substrates can be avoided under the laser irradiation because of the solvent protection.[10] Finally, it has vast practical applications, such as scientific expedition, scene of crime, medical diagnosis, food safety and environment.

We utilized the UV-vis diffuse reflection absorption spectrum to further monitor the change process after silver nanoparticle film remixing with water. It can be seen from Fig. 1a that the surface plasmon peak of silver film is at about 400 nm, which is attributed to the quadrupole plasmon excitation in coupled nanoparticles.[11] When 5 μL of solvent/water is dropped on the dry silver film, the surface plasmon peak gradually red-shifts from 400 nm to about 480 nm (Fig. 1b), indicating the decrease in the interparticle separation. Generally, the larger the number of silver nanoparticles and the shorter the interparticle distance, the more the peak of SPR shifts toward the long-wavelength region. However, in the present case, the number of nanoparticles was fixed. So the number of particles should make no contribution to the red-shift of the quadrupole plasmon excitation. Thus, the red-shift behavior can only be attributed to shortening of the interparticle distance.[12] While the solvent volatilizes completely, the surface plasmon peak of silver comes back to 400 nm (Fig. 1c). Ultimately, the UV-vis diffuse reflection absorption spectrum of Ag nanoparticles with an absorption maximum is at about the same location. During the volatilization process, the spectra differ strongly from the dry state film. It seems quite likely that the capillary forces increase significantly while the solvent is remixed, as particles rearrange and the number of close contacts increases.[13] Computer simulations establish that a combined short-range attraction and long-range repulsion can efficiently maintain such locally planar geometry.[6] In our study, the driving force for self-assembly into clusters is short-range attraction coming from the solvent capillary forces (Fig. 1e), which effectively acts as surface tension leading to a decrease in surface energy upon aggregation. On the other hand, cluster growth is limited by the increasing electrostatic energy of the clusters, which counterbalances the gain in surface energy. This balance between short-range attraction and long-range Coulomb repulsion provides a stabilizing mechanism against gelation and determines a finite aggregation number. A combination of short-range attraction and long-range repulsion resulting in the formation of small equilibrium clusters was also demonstrated in protein solutions and colloid–polymer mixtures systems.[14] When the film was transformed into a dry state, the short-range attraction of the solvent capillary forces disappeared completely. Thus, the silver nanoparticles come back to the original positions (Fig. 1f).

To elaborate the principle of MSNERS, we carried out a study on the Raman scattering intensity by theoretical calculation of the discrete dipole approximation (DDA) method. In simulated experiments, we observed the SPR peak shifts from 400 nm to 480 nm while the water is dropped. This indicates that the nanospheres are getting nearer in this process from 5.52 nm to 4.65 nm (Fig. 2a and b). The calculated results reveal that the magnitude of the maximally enhanced electric field is about 11.5 times greater for the 5.52 nm gap and about 43.7 times greater for the 4.65 nm gap than that of the incident light (Fig. 2c); the highest enhancement of Raman scattering appears at the junction between the particle and the substrate as hot spots with magnitudes of about 1.7×10^4 and 3.65×10^6 fold, respectively. The calculation results show that the gap shortens 0.87 nm during the volatilization process, which can improve at least 208 fold compared with the dry state.

Besides the SPR of MSNERS, we suppose solvent acted as an initiator and porter in our detection strategy, activating the target molecules and transporting the inactive-molecule to the effective region of the laser focus. The laser coming from the Raman instrument plays a critical role in providing the driving force for our detection system.[15] It can improve the detection sensitivity of target molecules. Another possible explanation is based on the refractive index change from air ($n \approx 1$) to water ($n \approx 1.33$). With an increase in the medium refractive index (RI), the frequency of the localized surface plasmon resonance (LSPR) red shifts.[16–18] Increasing RI can improve the intensity of Raman signals.

MSNERS has extraordinary potential for characterizing molecular structures such as drugs, particularly cocaine, which is vitally important for drug enforcement, especially as the use of these illicit substances is increasing. Though SERS is able to identify the above analyte substances uniquely, the detection limit of this type of sample is only about 10^{-5} M in former studies.[19] Most important, MSNERS is suitable for a reliable,

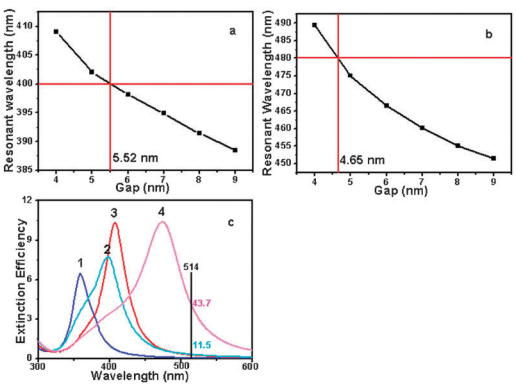

Fig. 2 Simulated result of the gap of silver dimer (36 nm) dependent the resonant wavelengths in air (a) and in water (b). Simulations of the extinction spectra based on DDA method for 36 nm silver nanospheres with different medium (c). Curve 1, single Ag sphere in air; curve 2, Ag spheres dimer with gap 5.52 nm in air; curve 3, single Ag sphere in water; curve 4, Ag spheres dimer with gap 4.65 nm in water. The black line is for the wavelength of 514 nm.

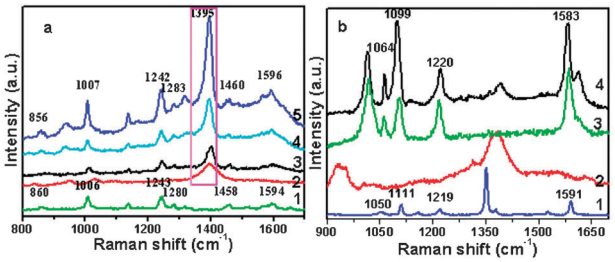

Fig. 3 Spectra of cocaine (a): Curve 1, Raman spectrum of solid cocaine. Curves 2 and 3, SERS spectra at different concentrations (2: 10^{-6} M, 3: 10^{-5} M) following the traditional SERS protocol; curves 4 and 5, MSNERS spectra at 10^{-8} M and 10^{-6} M, respectively. Spectra of methyl-parathion (b): Curve 1, Raman spectrum of solid. Curves 2 and 3, SERS spectra at different concentrations (2: 10^{-7} M, 3: 10^{-6} M) following the traditional SERS protocol; curve 4, MSNERS spectra at 10^{-8} M. Laser power on the sample was 1 mW, and the collection times were 5 s.

quick and, with respect to the cost of preparation, reasonable method of analysis. Fig. 3a shows that the normal Raman spectrum of pure cocaine HCl has several characteristic features that can be used to identify the drug, such as the aromatic ring (C=C) stretch at 1594 cm^{-1}, aromatic ring breathing mode at 1006 cm^{-1}, pyrrolidine ring (C–C) stretch at 860 cm^{-1} [20] and the weaker bands around 1275 and 1450 cm^{-1} to the tropane moiety (curve 1 of Fig. 3a).[21] It is quite difficult to acquire the SERS signal of cocaine HCl following the traditional SERS method in the dry state, when the concentration is lower than 10^{-6} M (curves 2 and 3 of Fig. 3a). Comparing curve 2 with curve 3, we conclude that the detection limit is 10^{-5} M. However, using MSNERS, cocaine HCl can be detected at 10^{-8} M (curve 4 and curve e of Fig. 3a), which suggests that MSNERS is a very simple and effective approach compared with the previous studies. The intense peaks from curve 2 to curve 5 at 1395 cm^{-1} came from the carbon signal caused by the Raman laser. The above experimental results provide an effective method for detecting the liquid drug residue of the drug-taking scene.

Recently, environmental problems have drawn more and more attention to the organic pollutants related to wastewater and polluted food. MSNERS can also be used for inspecting pesticide residues accurately and rapidly, such as the organophosphate pesticide methyl-parathion (MP). MSNERS can improve the detection limit of MP by two orders of magnitude ranged from 10^{-6} M to 10^{-8} M, and deserves to be recommended for improving the SERS development dilemma compared with high labor and cost consumption of optimizing the materials preparation and substrate fabrication. As shown in the Fig. 3b, the SERS spectrum of MP (curve 3) is similar to the solid ones (curve 1). The MSNERS spectrum of MP is also similar to the SERS spectrum. A detailed assignment of the spectral features has been reported in our former studies[22] and will not be repeated here.

In summary, an extremely simple and sensitive approach named MSNERS for Raman signal detection is proposed. The spectrum of MSNERS can be described as the Raman signal acquired by an ordinary SERS substrate with solvent/water volatilization during the detection process. Theoretical calculation by the DDA method showed that the detection limit can be improved by two to three orders of magnitude which is demonstrated by detection of cocaine and the organophosphate pesticide methyl-parathion. This ultrasensitive SERS might facilitate the measurement of a wider range of analytes including enzyme measurements[23] at lower concentration and with a short detection time.

We thank B. Ren and D. Wu for discussions. This work was supported by the National Basic Research Program of China (2007CB936603 and 2011CB933700), Hi-tech Research and Development Program of China (2009AA03Z330), and the Important Projects of Anhui Provincial Education Department (KJ2010ZD09).

Notes and references

1 (*a*) W. C. K. Poon, F. Renth, R. M. L. Evans, D. J. Fairhurst, M. E. Cates and P. N. Pusey, *Phys. Rev. Lett.*, 1999, **83**, 1239–1242; (*b*) A. Imhof and D. J. Pine, *Nature*, 1997, **389**, 948; (*c*) V. J. Anderson and H. N. W. Lekkerkerker, *Nature*, 2002, **416**, 811–815.
2 V. N. Manoharan, M. T. Elsesser and D. J. Pine, *Science*, 2003, **301**, 483–487.
3 E. M. Herzig, K. A. White, A. B. Schofield, W. C. K. Poon and P. S. Clegg, *Nat. Mater.*, 2007, **6**, 966–971.
4 K. Stratford, R. Adhikari, I. Pagonabarraga, J.-C. Desplat and M. E. Cates, *Science*, 2005, **309**, 2198–2201.
5 C. Chiu and H. Wang, *Phys. Rev. B: Condens. Matter Mater. Phys.*, 2007, **75**, 125416.
6 F. Sciortino, P. Tartaglia and E. Zaccarelli, *J. Phys. Chem. B*, 2005, **109**, 21942–21953.
7 A. I. Campbell, V. J. Anderson, J. S. van Duijneveldt and P. Bartlett, *Phys. Rev. Lett.*, 2005, **94**, 208301.
8 E. Sanz, K. A. White, P. S. Clegg and M. E. Cates, *Phys. Rev. Lett.*, 2009, **103**, 255502.
9 S.-Y. Chen, J. J. Mock, R. T. Hill, A. Chilkoti, D. R. Smith and A. A. Lazarides, *ACS Nano*, 2010, **4**, 6535–6546.
10 P. L. Stiles, J. A. Dieringer, N. C. Shah and R. P. Van Duyne, *Annu. Rev. Anal. Chem.*, 2008, **1**, 601–626.
11 T. Jensen, L. Kelly, A. Lazarides and G. C. Schatz, *J. Cluster Sci.*, 1999, **10**, 295–317.
12 M. Wang, Y. Li, Z. Xie, C. Liu and E. S. Yeung, *Mater. Chem. Phys.*, 2010, **119**, 153–157.
13 E. Kim, K. Stratford, R. Adhikari and M. E. Cates, *Langmuir*, 2008, **24**, 6549–6556.
14 A. Stradner, H. Sedgwick, F. Cardinaux, W. C. K. Poon, S. U. Egelhaaf and P. Schurtenberger, *Nature*, 2004, **432**, 492–495.
15 Y. Wang, H. Chen, S. Dong and E. Wang, *J. Raman Spectrosc.*, 2007, **38**, 515–521.
16 A. J. Haes and R. P. Van Duyne, *J. Am. Chem. Soc.*, 2002, **124**, 10596–10604.
17 P. K. Jain and M. A. El-Sayed, *J. Phys. Chem. C*, 2007, **111**, 17451–17454.
18 P. K. Jain, W. Qian and M. A. El-Sayed, *J. Am. Chem. Soc.*, 2006, **128**, 2426–2433.
19 B. Sagmuller, B. Schwarze, G. Brehm, G. Trachta and S. Schneider, *J. Mol. Struct.*, 2003, **661–662**, 279–290.
20 (*a*) A. P. Gamot, G. Vergoten and G. Fleury, *Talanta*, 1985, **32**, 363–372; (*b*) E. M. A. Ali, H. G. M. Edwards, M. D. Hargreaves and I. J. Scowen, *Anal. Chim. Acta*, 2008, **615**, 63–72.
21 M. D. Hargreaves, K. Page, T. Munshi, R. Tomsett, G. Lynch and H. G. M. Edwards, *J. Raman Spectrosc.*, 2008, **39**, 873–880.
22 (*a*) X. Li, G. Chen, L. Yang, Z. Jin and J. Liu, *Adv. Funct. Mater.*, 2010, **20**, 2815–2824; (*b*) J. Li, Y. Huang, Y. Ding, Z. Yang, S. Li, X. Zhou, F. Fan, W. Zhang, Z. Zhou, D. Wu, B. Ren, Z. Wang and Z. Tian, *Nature*, 2010, **464**, 392–395.
23 I. A. Larmour, K. Faulds and D. Graham, *Chem. Sci.*, 2010, **1**, 151–160.